

Holographic fabricated continuous wave operation of distributed feedback quantum cascade lasers at $\lambda \approx 8.5 \mu\text{m}^*$

Zhang Jinchuan(张锦川)^{1,2}, Wang Lijun(王利军)^{1,†}, Zhang Wei(张伟)¹, Liu Wanfeng(刘万峰)¹, Liu Junqi(刘俊岐)¹, Liu Fengqi(刘峰奇)¹, Li Lu(李路)¹, and Wang Zhanguo(王占国)¹

¹Key Laboratory of Semiconductor Materials Science, Institute of Semiconductors, Chinese Academy of Sciences, Beijing 100083, China

²Department of Electronic Engineering, Tsinghua University, Beijing 100084, China

Abstract: The fabrication and characterization of distributed feedback (DFB) quantum cascade lasers emitting at $\lambda \approx 8.5 \mu\text{m}$ are reported. The first-order DFB grating structure was defined using the holographic lithography technique. Reliable dynamic single-mode emission with a side-mode suppression ratio of 20 dB and a tuning coefficient of $-0.277 \text{ cm}^{-1}/\text{K}$ from 93 to 210 K is obtained in continuous wave mode by using high-reflectivity coating on the rear facet. The output power is over 100 mW at a temperature of 80 K.

Key words: quantum cascade laser; distributed feedback; holographic; continuous wave

DOI: 10.1088/1674-4926/32/4/044008

PACC: 4260F

1. Introduction

The quantum cascade laser (QCL) is one of the most promising light sources for the mid- and far-infrared wavelength range because of its high performance and compact size, and it is expected to find a variety of applications, such as gas sensing and high-resolution spectroscopy. These applications require a QCL with single-mode, high output power, continuous wave (CW) operation and a large tuning range with a narrow spectral linewidth^[1]. As a result, distributed feedback (DFB) QCLs have been demonstrated over a wide wavelength range ($3.5\text{--}16 \mu\text{m}$)^[2–5]. However, these devices are usually achieved with electron-beam lithography (EBL), which would limit the wide application of the DFB structure as a result of its rather expensive and time-consuming preparation procedure. Currently, only a few groups have realized room temperature CW operation of DFB QCLs in the long wavelength range ($\lambda > 8 \mu\text{m}$)^[6,7]. In those works, EBL was used for the fabrication of the grating, which is not so efficient. For the commercialization of DFB-QCLs, a holographic fabricated grating should be a better choice. In this paper, we apply holographic lithography (HL) to the fabrication of DFB QCLs at $\lambda \approx 8.5 \mu\text{m}$. Single-mode emission with a side-mode suppression ratio (SMSR) of about 20 dB is achieved up to temperatures of above 210 K in CW operation.

2. Device fabrication

The QCL structure was grown by solid-source molecular beam epitaxy on an n-InP (Si, $3 \times 10^{17} \text{ cm}^{-3}$) substrate. A $1.55\text{--}\mu\text{m}$ active region was sandwiched between two 300-nm-thick InGaAs layers. The first-order DFB grating with a period of $\Lambda = 1.4 \mu\text{m}$ (duty cycle of 50%) was defined on the upper

InGaAs layer using the HL technique and transferred by reactive ion etching in Ar/H₂/CH₄ plasma to a depth of about 80 nm. Then a $2\text{--}\mu\text{m}$ InP cladding layer and a $0.5\text{--}\mu\text{m}$ heavily-doped InP contact were grown directly on top of the grating region by metal-organic chemical-vapor deposition. The scanning electron microscope (SEM) image of the cross section of the DFB-QCL structure is shown in Fig. 1.

After growth, the wafer was etched into a double-channel waveguide laser with an average core width of $17.5 \mu\text{m}$ using conventional photolithography and nonselective wet chemical etching in HBr:HNO₃:H₂O solution. A 350-nm-thick SiO₂ layer was deposited by chemical vapor deposition for insulation around the ridges and electrical contacts were provided by a Ti/Au layer. An additional $5\text{--}\mu\text{m}$ -thick gold layer was subsequently electroplated to further improve heat dissipation. The device was finally thinned down to $170 \mu\text{m}$ and back contacts

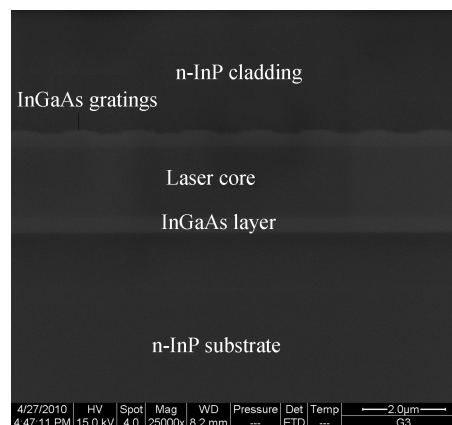


Fig. 1. SEM image of a cross-sectional view of the DFB-QCL structure.

* Project supported by the National Research Projects of China (Nos. 60525406, 60736031, 60806018, 60906026, 2006CB604903, 2007AA03Z446, 2009AA03Z403).

† Corresponding author. Email: ljwang@semi.ac.cn

Received 12 October 2010, revised manuscript received 8 November 2010

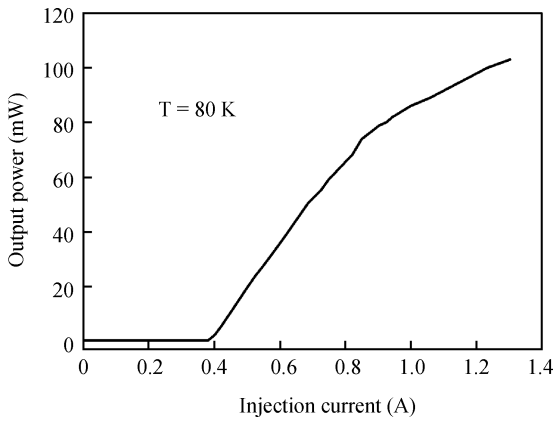


Fig. 2. Light–current characteristics at a heat sink temperature of 80 K measured in CW mode.

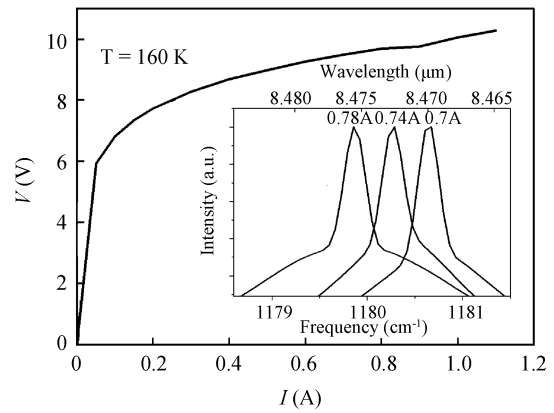


Fig. 4. $V-I$ curve at 160 K at CW injection currents. The inset shows single mode emission spectra in CW operation mode. The spectra are obtained at an injection current of 0.7, 0.74 and 0.78 A at 160 K.

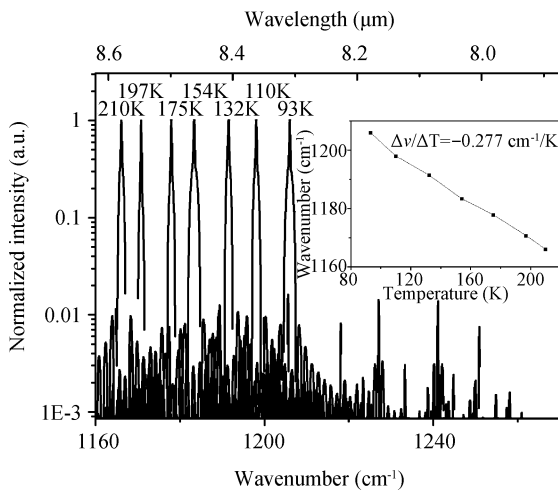


Fig. 3. Emission spectra of a device with a 17.5- μm -wide and 2-mm-long cavity in CW mode.

were formed with Ge/Au/Ni/Au. The lasers were mounted inside a liquid nitrogen cooled cryostat. Testing was performed on 2-mm-long devices with a high-reflectivity coating on the rear facet consisting of $\text{Al}_2\text{O}_3/\text{Ti}/\text{Au}/\text{Al}_2\text{O}_3$ (200/10/100/120 nm), which is deposited by electron-beam evaporation and has an estimated reflectivity of over 95%.

3. Results and discussion

The emitted optical power from the uncoated facet of the laser was measured with a calibrated thermopile detector placed directly in front of the laser facet. Figure 2 shows the typical light–current ($L-I$) characteristics of a DFB device with a 17.5- μm -wide and 2-mm-long cavity at a heat sink temperature of 80 K. The output power of 102 mW is obtained with a threshold current density (J_{th}) of 1.143 kA/cm^2 .

Figure 3 shows the normalized emission spectra of a DFB laser obtained for the temperature range of 93–210 K with a side-mode suppression ratio (SMSR) of 20 dB. The measurements were performed in CW mode using a Fourier transform infrared (FTIR) spectrometer. The emission peak was observed to shift from 1206.1 cm^{-1} at 93 K to 1166.1 cm^{-1} at 210 K,

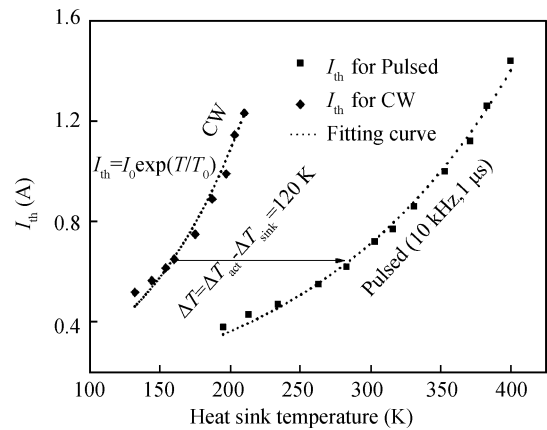


Fig. 5. Threshold current as a function of heat sink temperature in CW and pulsed modes of a 2-mm-long and 17.5- μm -wide DFB laser. The dashed line is the fitting result using the usual exponential function $J_{\text{th}} = J_0 \exp(T/T_0)$.

corresponding to a temperature tuning coefficient of $-0.277 \text{ cm}^{-1}/\text{K}$. The inset of Fig. 3 shows the linear tuning characteristics of the wavelength with temperature.

The voltage–current ($V-I$) curve is shown in Fig. 4. The threshold voltage of 9.42 V was measured at a temperature of 160 K. The inset of Fig. 4 shows the emission spectra of the same DFB laser, obtained at different currents of 0.7 A, 0.74 A and 0.78 A at 160 K in CW operation. The shift of the peak position indicates frequency tuning from 1180.64 to 1179.86 cm^{-1} . A tuning coefficient of $\Delta\nu/\Delta P = -0.895 \text{ cm}^{-1}\text{W}^{-1}$ is obtained from the frequency and the electrical input power. The peak shift is attributed to the thermal variation of the optical waveguide’s refractive index due to heating by the current. The thermal resistance (R_{th}) of the DFB laser can be estimated using the temperature and current tuning rates $R_{\text{th}} = \Delta\nu/\Delta P \times (\Delta\nu/\Delta T)^{-1}$ with the assumption that the temperature is fairly uniform^[8]. Inserting the above tuning rates, we get a thermal resistance of 3.23 K/W in the temperature range between 93 K and 210 K.

Figure 5 illustrates the lasing threshold current at the corresponding heatsink temperatures in CW and pulsed modes of the same 2-mm-long and 17.5- μm -wide DFB laser. The dashed

line is the fitting result using the usual exponential function $J_{\text{th}} = J_0 \exp(T/T_0)$. The characteristic temperature (T_0) was 160 K for pulsed operation between 194 K and 400 K. Generally, the heat dissipation from the active region during CW operation is insufficient and the laser active region temperature T_{act} is typically much higher than the heatsink temperature T_{sink} ^[9]. As a result, the threshold current increases more rapidly with a higher value in CW mode than in pulsed mode as the temperature is increased. From 132 to 210 K, T_0 reduces to 95 K in CW mode.

The dependence of the threshold current density J_{th} on the actual core temperature T_{act} of the laser is measured in pulsed mode at low duty cycles, where heating effects are negligible (that is, $T_{\text{act}} - T_{\text{sink}}$). At 160 K, the thermal resistance of the laser, which is defined as $R_{\text{th}} = (T_{\text{act}} - T_{\text{sink}})/V_{\text{th}}I_{\text{th}}$, can also be determined by knowing the dissipated electrical power at threshold in CW mode. At threshold, the effective temperature difference between the active region T_{act} and the heat sink temperature T_{sink} is 120 K from Fig. 5. For CW operation at 160 K, $I_{\text{th}} = 0.68$ A and $V_{\text{th}} = 9.42$ V. This leads to a thermal resistance value of $R_{\text{th}} = 18.73$ K/W for the 2-mm-long and 17.5- μm -wide DFB laser. This higher value of R_{th} , as compared to the value obtained from the spectral tuning, is likely due to the fact that the threshold current density is more sensitive to local temperature changes in the laser active core while the spectral tuning relies on an overall change in the refractive index across the entire laser^[8, 10]. This result indicates that more work on processing to enhance the heat dissipation is required to realize room temperature CW operation.

4. Conclusion

In conclusion, we have demonstrated the CW performance of single-mode DFB QCLs operating at $\lambda \approx 8.5$ μm up to temperatures of above 210 K with a SMSR ≥ 20 dB. The HL technique is shown to be a very effective method to define DFB gratings, which will be significant in the large-scale fabrication

of DFB-QCLs.

Acknowledgements

The authors would like to acknowledge Liang Ping and Hu Ying for their help with device fabrication.

References

- [1] Kosterev A, Tittel F. Chemical sensors based on quantum cascade Lasers. *IEEE J Quantum Electron*, 2002, 38: 582
- [2] Köhler R, Gmachl C, Capasso F, et al. Single-mode tunable, pulsed, and continuous wave quantum-cascade distributed feedback lasers at $\lambda \approx 4.6\text{--}4.7$ μm . *Appl Phys Lett*, 2000, 76: 1092
- [3] Gmachl C, Straub A, Colombelli R, et al. Single-mode, tunable distributed-feedback and multiple-wavelength quantum cascade lasers. *IEEE J Quantum Electron*, 2002, 38: 569
- [4] Aellen T, Blaser S, Beck M, et al. Continuous-wave distributed-feedback quantum-cascade lasers on a Peltier cooler. *Appl Phys Lett*, 2003, 83: 1929
- [5] Rochat M, Hofstetter D, Beck M, et al. Long-wavelength ($\lambda \approx 16$ μm), room-temperature, single-frequency quantum-cascade lasers based on a bound-to-continuum transition. *Appl Phys Lett*, 2001, 79: 4271
- [6] Darvish S R, Slivken S, Evans A, et al. Room-temperature, high-power, and continuous-wave operation of distributed-feedback quantum cascade lasers at $\lambda \approx 9.6$ μm . *Appl Phys Lett*, 2006, 88: 201114
- [7] Wittmann A, Bonetti Y, Fischer M, et al. Distributed-feedback quantum cascade lasers at 9 μm operating in continuous wave up to 423 K. *IEEE Photonics Technol Lett*, 2009, 21: 12
- [8] Darvish S R, Zhang W, Evans A, et al. High-power, continuous-wave operation of distributed-feedback quantum-cascade lasers at $\lambda \approx 7.8$ μm . *Appl Phys Lett*, 2006, 89: 251119
- [9] Beck M, Hofstetter D, Aellen T, et al. Continuous wave operation of a mid-infrared semiconductor laser at room temperature. *Science*, 2002, 295: 302
- [10] Blaser S, Yarekha D A, Hvozdar L, et al. Room-temperature, continuous-wave, single-mode quantum-cascade lasers at $\lambda \approx 5.4$ μm . *Appl Phys Lett*, 2005, 86: 041109